Measurements of B→D[over ¯]D_{s0}^{*+}(2317) decay rates and a search for isospin partners of the D_{s0}^{*+}(2317)

S.-K. Choi *et al.* (The Belle Collaboration)

Phys. Rev. D **91**, 092011 — Published 28 May 2015

DOI: 10.1103/PhysRevD.91.092011

Measurements of $B \to \bar{D}D_{s0}^{*+}(2317)$ decay rates and a search for isospin partners of the $D_{s0}^{*+}(2317)$

S.-K. Choi,[10] S. L. Olsen,[18] A. Abdesselam,[57] I. Adachi,[13,9] H. Aihara,[62] K. Arinstein,[4] D. M. Asner,[48] T. Aushev,[38,22] R. Ayad,[57] V. Babu,[58] I. Badhrees,[57,27] A. M. Bakich,[56] E. Barberio,[36] V. Bhardwaj,[54] B. Bhuyan,[15] G. Bonvicini,[67] A. Bozek,[45] M. Bračko,[34,23] T. E. Browder,[12] D. Červenkov,[5] A. Chen,[42] B. G. Cheon,[11] K. Chilikin,[22] R. Chistov,[22] K. Cho,[28] V. Chobanova,[35] Y. Choi,[55] D. Cinabro,[67] J. Dalseno,[35,59] M. Danilov,[22,37] Z. Doležal,[5] Z. Drásal,[5] A. Drutskoy,[22,37] D. Dutta,[58] S. Eidelman,[4] H. Farhat,[67] J. E. Fast,[48] T. Ferber,[7] B. G. Fulsom,[48] V. Gaur,[58] N. Gabyshev,[4] A. Garmash,[4] D. Getzkow,[8] R. Gillard,[67] R. Glattauer,[19] Y. M. Goh,[11] B. Golob,[32,23] J. Haba,[13,9] T. Hara,[13,9] K. Hayasaka,[40] H. Hayashii,[41] X. H. He,[49] T. Horiguchi,[61] W.-S. Hou,[44] T. Iijima,[40,39] K. Inami,[39] G. Inguglia,[7] A. Ishikawa,[61] R. Itoh,[13,9] Y. Iwasaki,[13] I. Jaegle,[12] D. Joffe,[26] T. Julius,[36] K. H. Kang,[30] E. Kato,[61] P. Katrenko,[22] T. Kawasaki,[46] B. H. Kim,[52] D. Y. Kim,[53] H. J. Kim,[30] J. B. Kim,[29] J. H. Kim,[28] K. T. Kim,[29] S. H. Kim,[11] Y. J. Kim,[28] K. Kinoshita,[6] B. R. Ko,[29] P. Kodyš,[5] S. Korpar,[34,23] P. Križan,[32,23] P. Krokovny,[4] T. Kumita,[64] A. Kuzmin,[4] Y.-J. Kwon,[69] J. S. Lange,[8] I. S. Lee,[11] P. Lewis,[12] H. Li,[17] L. Li Gioi,[35] J. Libby,[16] P. Lukin,[4] D. Matvienko,[4] K. Miyabayashi,[41] H. Miyata,[46] R. Mizuk,[22,37] G. B. Mohanty,[58] A. Moll,[35,59] H. K. Moon,[29] T. Mori,[39] R. Mussa,[21] E. Nakano,[47] M. Nakao,[13,9] T. Nanut,[23] Z. Natkaniec,[45] M. Nayak,[16] N. K. Nisar,[58] S. Nishida,[13,9] S. Ogawa,[60] S. Okuno,[24] P. Pakhlov,[22,37] G. Pakhlova,[38,22] B. Pal,[6] C. W. Park,[55] H. Park,[30] T. K. Pedlar,[33] L. Pesántez,[3] R. Pestotnik,[23] M. Petrič,[23] L. E. Piilonen,[66] E. Ribežl,[23] M. Ritter,[35] A. Rostomyan,[7] S. Ryu,[52] Y. Sakai,[13,9] S. Sandilya,[58] L. Santelj,[13] T. Sanuki,[61] Y. Sato,[39] V. Savinov,[50] O. Schneider,[31] G. Schnell,[1,14] C. Schwanda,[19] K. Senyo,[68] M. E. Sevior,[36] M. Shapkin,[20] V. Shebalin,[4] C. P. Shen,[2] T.-A. Shibata,[63] J.-G. Shiu,[44] B. Shwartz,[4] A. Sibidanov,[56] F. Simon,[35,59] Y.-S. Sohn,[69] A. Sokolov,[20] E. Solovieva,[22] M. Starič,[23] M. Steder,[7] U. Tamponi,[21,65] S. Tanaka,[13,9] K. Tanida,[52] Y. Teramoto,[47] V. Trusov,[25] M. Uchida,[63] T. Uglov,[22,38] Y. Unno,[11] S. Uno,[13,9] P. Urquijo,[36] Y. Usov,[4] C. Van Hulse,[1] P. Vanhoefer,[35] G. Varner,[12] A. Vinokurova,[4] V. Vorobyev,[4] A. Vossen,[17] M. N. Wagner,[8] C. H. Wang,[43] M.-Z. Wang,[44] X. L. Wang,[66] Y. Watanabe,[24] K. M. Williams,[66] E. Won,[29] S. Yashchenko,[7] Z. P. Zhang,[51] V. Zhilich,[4] V. Zhulanov,[4] and A. Zupanc[23]

(The Belle Collaboration)

[1]*University of the Basque Country UPV/EHU, 48080 Bilbao*
[2]*Beihang University, Beijing 100191*
[3]*University of Bonn, 53115 Bonn*
[4]*Budker Institute of Nuclear Physics SB RAS and Novosibirsk State University, Novosibirsk 630090*
[5]*Faculty of Mathematics and Physics, Charles University, 121 16 Prague*
[6]*University of Cincinnati, Cincinnati, Ohio 45221*
[7]*Deutsches Elektronen–Synchrotron, 22607 Hamburg*
[8]*Justus-Liebig-Universität Gießen, 35392 Gießen*
[9]*SOKENDAI (The Graduate University for Advanced Studies), Hayama 240-0193*
[10]*Gyeongsang National University, Chinju 660-701*
[11]*Hanyang University, Seoul 133-791*
[12]*University of Hawaii, Honolulu, Hawaii 96822*
[13]*High Energy Accelerator Research Organization (KEK), Tsukuba 305-0801*
[14]*IKERBASQUE, Basque Foundation for Science, 48013 Bilbao*
[15]*Indian Institute of Technology Guwahati, Assam 781039*
[16]*Indian Institute of Technology Madras, Chennai 600036*
[17]*Indiana University, Bloomington, Indiana 47408*
[18]*Center for Underground Physics, Institute for Basic Science, Daejeon 305-811*
[19]*Institute of High Energy Physics, Vienna 1050*
[20]*Institute for High Energy Physics, Protvino 142281*
[21]*INFN - Sezione di Torino, 10125 Torino*
[22]*Institute for Theoretical and Experimental Physics, Moscow 117218*
[23]*J. Stefan Institute, 1000 Ljubljana*
[24]*Kanagawa University, Yokohama 221-8686*
[25]*Institut für Experimentelle Kernphysik, Karlsruher Institut für Technologie, 76131 Karlsruhe*
[26]*Kennesaw State University, Kennesaw GA 30144*
[27]*King Abdulaziz City for Science and Technology, Riyadh 11442*
[28]*Korea Institute of Science and Technology Information, Daejeon 305-806*

[29]Korea University, Seoul 136-713
[30]Kyungpook National University, Daegu 702-701
[31]École Polytechnique Fédérale de Lausanne (EPFL), Lausanne 1015
[32]Faculty of Mathematics and Physics, University of Ljubljana, 1000 Ljubljana
[33]Luther College, Decorah, Iowa 52101
[34]University of Maribor, 2000 Maribor
[35]Max-Planck-Institut für Physik, 80805 München
[36]School of Physics, University of Melbourne, Victoria 3010
[37]Moscow Physical Engineering Institute, Moscow 115409
[38]Moscow Institute of Physics and Technology, Moscow Region 141700
[39]Graduate School of Science, Nagoya University, Nagoya 464-8602
[40]Kobayashi-Maskawa Institute, Nagoya University, Nagoya 464-8602
[41]Nara Women's University, Nara 630-8506
[42]National Central University, Chung-li 32054
[43]National United University, Miao Li 36003
[44]Department of Physics, National Taiwan University, Taipei 10617
[45]H. Niewodniczanski Institute of Nuclear Physics, Krakow 31-342
[46]Niigata University, Niigata 950-2181
[47]Osaka City University, Osaka 558-8585
[48]Pacific Northwest National Laboratory, Richland, Washington 99352
[49]Peking University, Beijing 100871
[50]University of Pittsburgh, Pittsburgh, Pennsylvania 15260
[51]University of Science and Technology of China, Hefei 230026
[52]Seoul National University, Seoul 151-742
[53]Soongsil University, Seoul 156-743
[54]University of South Carolina, Columbia, South Carolina 29208
[55]Sungkyunkwan University, Suwon 440-746
[56]School of Physics, University of Sydney, NSW 2006
[57]Department of Physics, Faculty of Science, University of Tabuk, Tabuk 71451
[58]Tata Institute of Fundamental Research, Mumbai 400005
[59]Excellence Cluster Universe, Technische Universität München, 85748 Garching
[60]Toho University, Funabashi 274-8510
[61]Tohoku University, Sendai 980-8578
[62]Department of Physics, University of Tokyo, Tokyo 113-0033
[63]Tokyo Institute of Technology, Tokyo 152-8550
[64]Tokyo Metropolitan University, Tokyo 192-0397
[65]University of Torino, 10124 Torino
[66]CNP, Virginia Polytechnic Institute and State University, Blacksburg, Virginia 24061
[67]Wayne State University, Detroit, Michigan 48202
[68]Yamagata University, Yamagata 990-8560
[69]Yonsei University, Seoul 120-749

We report improved measurements of the product branching fractions $\mathcal{B}(B^+ \to \bar{D}^0 D_{s0}^{*+}(2317)) \times \mathcal{B}(D_{s0}^{*+}(2317) \to D_s^+\pi^0) = (8.0^{+1.3}_{-1.2} \pm 1.1 \pm 0.4) \times 10^{-4}$ and $\mathcal{B}(B^0 \to D^- D_{s0}^{*+}(2317)) \times \mathcal{B}(D_{s0}^{*+}(2317) \to D_s^+\pi^0) = (10.2^{+1.3}_{-1.2} \pm 1.0 \pm 0.4) \times 10^{-4}$, where the first errors are statistical, the second are systematic and the third are from D and D_s^+ branching fractions. In addition, we report negative results from a search for hypothesized neutral ($\mathbf{z^0}$) and doubly charged ($\mathbf{z}^{++}$) isospin partners of the $D_{s0}^{*+}(2317)$ and provide upper limits on the product branching fractions $\mathcal{B}(B^0 \to D^0\mathbf{z^0}) \times \mathcal{B}(\mathbf{z^0} \to D_s^+\pi^-)$ and $\mathcal{B}(B^+ \to D^0\mathbf{z}^{++}) \times \mathcal{B}(\mathbf{z}^{++} \to D_s^+\pi^+)$ that are more than an order of magnitude smaller than theoretical expectations for the hypotheses that the $D_{s0}^{*+}(2317)$ is a member of an isospin triplet. The analysis uses a 711 fb^{-1} data sample containing 772 million $B\bar{B}$ meson pairs collected at the $\Upsilon(4S)$ resonance in the Belle detector at the KEKB collider.

PACS numbers: 12.39.Mk, 13.20.He, 14.40.Lb

I. INTRODUCTION

The $D_{s0}^{*+}(2317)$ meson, hereinafter referred to as the D_{s0}^{*+}, was first observed by BaBar as a narrow peak in the $D_s^+\pi^0$ invariant mass spectrum produced in inclusive $e^+e^- \to D_s^+\pi^0 X$ annihilation processes [1, 2], and confirmed by CLEO [3]. Its production in the B meson decay processes $B \to \bar{D}D_{s0}^{*+}$ was subsequently established by both Belle [4] and BaBar [5]. (Here, B and $\bar{D}$ are used to denote B^0 and D^- or B^+ and $\bar{D}^0$.) Although it is generally considered to be the conventional $I(J^P) = 0(0^+)$ P-wave $c\bar{s}$ meson, its mass, $M_{D_{s0}^{*+}} = 2317.8 \pm 0.6$ MeV [6, 7], is the same as the peak mass of its non-strange counterpart, the 0^+ P-wave $c\bar{q}$ ($q = u$ or d) D_0^* with mass

$M_{D_0^*} = 2318 \pm 29$ MeV [6], in spite of the fact that the mass of the s-quark is ~ 100 MeV above that of either of the q-quarks. Potential model [8] and lattice-QCD [9] calculations published prior to the BaBar discovery predicted that the 0^+ P-wave $c\bar{s}$ meson mass would be well above the $m_{D^0} + m_{K^+} = 2358.6$ MeV threshold and have a large partial decay width for the strong interaction allowed process $D_{s0}^{*+} \to DK$. The observation of a subthreshold mass has led to theoretical speculation that the D_{s0}^{*+} is not a simple $c\bar{s}$ meson, but instead a DK molecule [10], a diquark-diantiquark state [11] or some mixture of a $c\bar{s}$ core state with a DK molecule and/or a diquark-diantiquark [12].

A $c\bar{s}$ meson with mass below the 2358.6 MeV threshold would decay via the isospin-violating process $D_{s0}^{*+} \to D_s^+\pi^0$ or the electromagnetic process $D_{s0}^{*+} \to D_s^{*+}\gamma$ and, thus, have a narrow natural width. This is consistent with experimental measurements, which have established a 95% confidence level (CL) upper limit on the total width of $\Gamma_{D_{s0}^{*+}} \leq 3.8$ MeV [6]. The small width of the D_{s0}^{*+} is evidence for an $I = 0$ assignment. However, the CLEO experiment has established a stringent 90% CL upper limit on the partial width for $D_{s0}^{*+} \to D_s^+\gamma$ decay [3]:

$$R(D_{s0}^{*+}) \equiv \frac{\Gamma(D_{s0}^{*+} \to D_s^+\gamma)}{\Gamma(D_{s0}^{*+} \to D_s^+\pi^0)} \leq 0.059, \qquad (1)$$

while studies that consider the D_{s0}^{*+} to be the $c\bar{s}$ chiral partner of the D_s^+ [13] predict values for $R(D_{s0}^{*+})$ that are higher than the CLEO upper limit. Product branching fractions for $B \to \bar{D}D_{s0}^{*+}$, $D_{s0}^{*+} \to D_s^+\pi^0$ have been measured by BaBar [5] and Belle [4]; the PDG averages [6] of their results are:

$$\mathcal{B}(B^+ \to \bar{D}^0 D_{s0}^{*+}) \times \mathcal{B}(D_{s0}^{*+} \to D_s^+\pi^0) = (7.3^{+2.2}_{-1.7}) \times 10^{-4},$$
$$\mathcal{B}(B^0 \to D^- D_{s0}^{*+}) \times \mathcal{B}(D_{s0}^{*+} \to D_s^+\pi^0) = (9.7^{+4.0}_{-3.3}) \times 10^{-4}.$$

Under the plausible assumption that $\mathcal{B}(D_{s0}^{*+} \to D_s^+\pi^0) \sim 1$, these measurements translate into the branching fraction ratios

$$\frac{\mathcal{B}(B^+ \to \bar{D}^0 D_{s0}^{*+})}{\mathcal{B}(B^+ \to \bar{D}^0 D_s^+)} = 0.081^{+0.026}_{-0.021},$$
$$\frac{\mathcal{B}(B^0 \to D^- D_{s0}^{*+})}{\mathcal{B}(B^0 \to D^- D_s^+)} = 0.13^{+0.06}_{-0.05},$$

which the authors of Refs. [14] and [15] note are well below expectations for a purely $c\bar{s}$ quark-antiquark state and an indication of some kind of multiquark content.

The BaBar and Belle measurements for both B^+ and B^0 modes agree within errors, the biggest difference is 1.5σ for the B^0 mode. In both cases, the measurements are based on event samples that are about 20% of the currently available data. Updated measurements based on the full data sets from both experiments would be useful.

A report by Hayashigaki and Terasaki [16] concludes that an $I = 1$ and $I_3 = 0$ assignment for the D_{s0}^{*+} cannot be ruled out and claims, in fact, that an $I = 1$ diquark-diantiquark interpretation is favored by some existing data. If this were the case, doubly charged $I_3 = 1$ ($\mathbf{z}^{++}$) and neutral $I_3 = -1$ ($\mathbf{z}^{\mathbf{0}}$) partners of the D_{s0}^{*+} with mass within $\sim \pm 10$ MeV of $M_{D_{s0}^{*+}}$ should exist. Since the $\mathbf{z}^{++}$ and $\mathbf{z}^{\mathbf{0}}$ would be charmed mesons with $I = 1$ and $S = 1$, they would necessarily have a minimal quark content of $c\bar{s}u\bar{d}$ and $c\bar{s}d\bar{u}$, respectively. Although a BaBar search for doubly charged and neutral partners of the D_{s0}^{*+} in inclusive e^+e^- annihilation events sets 95% CL upper limits on their production rates at 1.7% and 1.3%, respectively, of that for the D_{s0}^{*+} [17], Terasaki has argued that these do not conclusively rule out their existence [18]. If the $\mathbf{z}^{++}$ and $\mathbf{z}^{\mathbf{0}}$ mesons exist, isospin invariance ensures that the product branching fractions $\mathcal{B}(B \to \bar{D}\mathbf{z}^{++,\mathbf{0}}) \times \mathcal{B}(\mathbf{z}^{++,\mathbf{0}} \to D_s^+\pi^{+,-})$ will be nearly equal to $\mathcal{B}(B \to \bar{D}D_{s0}^{*+}) \times \mathcal{B}(D_{s0}^{*+} \to D_s^+\pi^0)$.

Here, we report measurements of $\mathcal{B}(B^+ \to \bar{D}^0 D_{s0}^{*+}) \times \mathcal{B}(D_{s0}^{*+} \to D_s^+\pi^0)$ and $\mathcal{B}(B^0 \to D^- D_{s0}^{*+}) \times \mathcal{B}(D_{s0}^{*+} \to D_s^+\pi^0)$ using a data sample that is more than six times larger than used in previous results [4] and a search for doubly charged ($\mathbf{z}^{++}$) and neutral ($\mathbf{z}^{\mathbf{0}}$) isospin partners of the D_{s0}^{*+} in the decay processes $B^+ \to D^-\mathbf{z}^{++}$, $\mathbf{z}^{++} \to D_s^+\pi^+$ and $B^0 \to \bar{D}^0\mathbf{z}^{\mathbf{0}}$, $\mathbf{z}^{\mathbf{0}} \to D_s^+\pi^-$. The results are based on the full Belle $\Upsilon(4S)$ data sample (711 fb^{-1}) that contains 772 million $B\bar{B}$ meson pairs produced at a center-of-mass system (cms) energy of $\sqrt{s} = 10.58$ GeV and collected in the Belle detector at the KEKB energy-asymmetric e^+e^- collider [19].

II. DETECTOR DESCRIPTION

The Belle detector is a large-solid-angle magnetic spectrometer that consists of a silicon vertex detector, a 50-layer cylindrical drift chamber, an array of aerogel threshold Cherenkov counters, a barrel-like arrangement of time-of-flight scintillation counters, and an electromagnetic calorimeter comprised of CsI(Tl) crystals located inside a superconducting solenoid coil that provides a 1.5 T magnetic field. An iron flux-return located outside of the coil is instrumented to detect K_L mesons and to identify muons. The detector is described in detail elsewhere [20].

III. EVENT SELECTION

We reconstruct D_s^+ mesons via their $\pi^+K^+K^-$ decay mode, which has a branching fraction of $\mathcal{B}_{D_s^+} = (5.39 \pm 0.21)\%$, D^- mesons via the $K^+\pi^-\pi^-$ decay mode ($\mathcal{B}_{D^-} = (9.13 \pm 0.19)\%$) and $\bar{D}^0$ mesons via the $K^+\pi^-$ ($\mathcal{B}_{K\pi} = (3.88 \pm 0.05)\%$) and $K^+\pi^+\pi^-\pi^-$ ($\mathcal{B}_{K3\pi} = (8.08 \pm 0.20)\%$) decay modes [6].

For all charged particles, we require $dr < 0.7$ cm and $|dz| < 3.0$ cm, where dr and dz are the track's distances of closest approach to the run-dependent mean interaction point transverse to and parallel to the e^+ beam direction, respectively. Charged particle identification is accomplished by combining information from different detector subsystems to form likelihood ratios, $L_{K/\pi} = L_K/(L_K + L_\pi)$, where L_K (L_π) is the likelihood of the kaon (pion) [21]. A charged track is classified as a kaon (pion) if $L_{K/\pi(\pi/K)} > 0.5$, with both the muon likelihood ratio and electron likelihood smaller than 0.95. For $B^0 \to D^- D_{s0}^{*+}$ decay, the kaon and pion identification efficiencies both exceed 95%. We reconstruct π^0 mesons via their $\pi^0 \to \gamma\gamma$ decay mode using γ candidates with $E_\gamma > 30$ MeV and $\gamma\gamma$ combinations that satisfy a one-constraint (1C) kinematic fit to m_{π^0} with $\chi^2 < 6.0$. In addition, we require $|M_{\gamma\gamma} - m_{\pi^0}| < 12$ MeV and the π^0 three-momentum in the e^+e^- cms $p_{\pi^0}^{\mathrm{cms}} < 1.9$ GeV.

Candidate $\bar{D}$ mesons are required to have a $Kn\pi$ ($n = 1$ to 3) invariant mass in the range $|M_{Kn\pi} - m_D| < 2.5\sigma$ of the observed peak mass, where σ is the width from a Gaussian fit to the $Kn\pi$ invariant mass peak; D_s^+ candidates are required to be in the mass interval $|M_{K^+K^-\pi^+} - m_{D_s^+}| < 2.5\sigma$. Here, the values of σ range from 4.6 MeV to 5.5 MeV.

Candidate $B \to \bar{D} D_{s0}^{*+}$ decays are identified by: *i)* the cms energy difference $\Delta E \equiv E_B^{\mathrm{cms}} - E_{\mathrm{beam}}^{\mathrm{cms}}$; *ii)* the beam-energy constrained mass $M_{\mathrm{bc}} \equiv \sqrt{(E_{\mathrm{beam}}^{\mathrm{cms}})^2 - (p_B^{\mathrm{cms}})^2}$; and *iii)* the $D_s^+\pi^0$ invariant mass. Here $E_{\mathrm{beam}}^{\mathrm{cms}}$ is the cms beam energy and E_B^{cms} and p_B^{cms} are the total cms energy and three-momentum of the particles forming the $\bar{D} D_{s0}^{*+}$ combination. We select events with $M_{\mathrm{bc}} > 5.20$ GeV, -0.12 GeV $< \Delta E <$ 0.1 GeV and 2.228 GeV $< M_{D_s^+\pi^0} <$ 2.418 GeV for three-dimensional fitting, and define signal regions as $|M_{\mathrm{bc}} - m_B| <$ 0.007 GeV, -0.033 GeV $< \Delta E <$ 0.030 GeV and $|M_{D_s^+\pi^0} - 2.3178\ \mathrm{GeV}| < 0.015$ GeV. For candidate $B \to \bar{D}\mathbf{z}^{++}$ ($\mathbf{z^0}$) decays, the π^0 is replaced by a π^+ (π^-) and the ΔE signal region is compressed to $|\Delta E| < 0.023$ GeV. These intervals correspond approximately to $\pm 2.5\sigma$ windows around the central values for each variable.

To reduce background from $e^+e^- \to q\bar{q}$ continuum processes, where $q = u, d, s, c$, we require: $R_2 < 0.3$, where R_2 is the normalized second Fox-Wolfram moment [22]; $|\cos\theta_B| < 0.8$, where θ_B is the polar angle of the candidate B-meson direction in the cms; and $|\cos\theta_{\mathrm{thr}B}| < 0.8$, where $\theta_{\mathrm{thr}B}$ is the cms angle between the thrust axis of the B candidate and that of the remaining unused tracks in the event. These requirements reject 14% of $B^0 \to D^- D_{s0}^{*+}$ signal and 45% of $q\bar{q}$ continuum.

IV. MC SIMULATION

We use Monte Carlo (MC) simulation to optimize selection criteria, determine acceptance and study multiple candidates per event [23]. We generate signal MC for each process under investigation using PDG values [6] for sub-decay branching fractions and setting $\mathcal{B}(D_{s0}^{*+} \to D_s^+\pi^0)$ and $\mathcal{B}(\mathbf{z}^{++,\mathbf{0}} \to D_s^+\pi^{+,-}) = 1$. In addition, we use a generic $B\bar{B}$ MC sample with about three times the integrated luminosity of the actual data sample to investigate possible peaking backgounds. The simulated events are processed through the same reconstruction and selection codes that are used for the real data.

V. MULTIPLE CANDIDATES

The $D_{s0}^{*+} \to D_s^+\pi^0$ mode is plagued by a large fraction of events with multiple candidates. The numbers of events with multiple entries in the full fitted region are summarized in Table I. Since the MC samples reproduce the data reasonably well, we use the MC as a guide for methods to reduce the multiple candidates.

TABLE I: Fractions of multiple candidate events in data and MC.

Sample	$B^0 \to D^- D_{s0}^{*+}$ $D^- \to K\pi\pi$	$B^+ \to \bar{D}^0 D_{s0}^{*+}$ $\bar{D}^0 \to K\pi$	$B^+ \to \bar{D}^0 D_{s0}^{*+}$ $\bar{D}^0 \to K3\pi$
Sig. MC	70%	45%	70%
$B\bar{B}$ MC	69%	39%	69%
Data	68%	39%	69%

For the $D^- \to K^+\pi^-\pi^-$ and $\bar{D}^0 \to K^+\pi^+\pi^-\pi^-$ modes, about two thirds of the multiple candidates are low energy photons forming multiple $\pi^0 \to \gamma\gamma$ combinations and one third are multiple charged pions in the D candidate. For the $\bar{D}^0 \to K^+\pi^-$ mode, essentially all of the multiple candidates are associated with the $\pi^0 \to \gamma\gamma$ reconstruction.

We use the $\gamma\gamma$ energy asymmetry, $E_{\mathrm{asym}} \equiv (E_1 - E_2)/(E_1 + E_2)$, where E_1 (E_2) is the higher (lower) energy photon of the $\gamma\gamma$ pair, to select π^0 candidates. Figure 1(left) shows the E_{asym} distribution for correctly assigned $\gamma\gamma$ pairs in signal MC events; the right panel in the same figure shows the same distribution for incorrectly assigned combinations. Here, the events are required to be in the M_{bc} and ΔE signal regions. According to MC studies, the strong peak near $E_{\mathrm{asym}} \simeq 0.85$ in the incorrect-assignment plot is mostly due to beam-produced background photons. Figure 2 shows the corresponding χ^2 distributions from the $\pi^0 \to \gamma\gamma$ kinematic fits. To reduce the γ-associated multiple candidates while minimizing loss of signal efficiency, we require that photons in the energy interval 30 MeV $< E_\gamma <$ 40 MeV have $\chi^2 < 0.5$ for the 1C fit or $E_{\mathrm{asym}} < 0.7$. For remaining events with multiple γ candidates, we select the combination with the smallest E_{asym} value. For multiple $\bar{D}$ (D_s^+) candidates, we select the track combination with invariant mass closest to the PDG value for m_D ($m_{D_s^+}$).

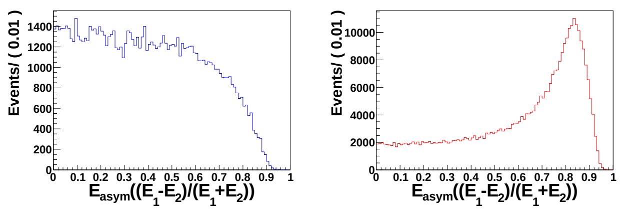

FIG. 1: The $E_{\rm asym}$ distributions for signal MC events for correctly **(left)** and incorrectly **(right)** assigned photons.

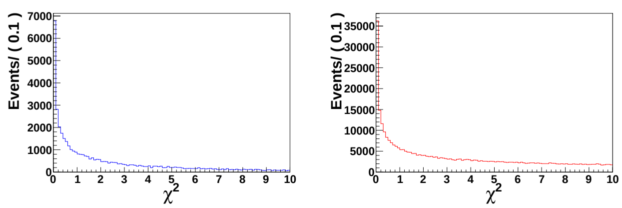

FIG. 2: The χ^2 distributions from the $\pi^0 \to \gamma\gamma$ fit for signal MC events for correctly **(left)** and incorrectly **(right)** assigned photons.

VI. $\bar{D}D_{S0}^{*+}$ EFFICIENCIES

We determine event yields from unbinned three-dimensional likelihood fits ($M_{\rm bc}$ *vs.* $M(D_s^+\pi^0)$ *vs.* ΔE) to the selected data using a bifurcated Gaussian function for the $M_{\rm bc}$ signal probability density function (PDF) and an ARGUS function [24] multiplied by a second-order Chebyshev polynomial for the $M_{\rm bc}$ combinatorial-background PDF. For ΔE, we use a Crystal Ball function [25] for the signal PDF and a third-order Chebyshev polynomial for the combinatorial-background PDF. For $M(D_s^+\pi^0)$, we use a Gaussian function for the signal PDF and a third-order Chebyshev polynomial for the combinatorial-background PDF.

In the generic $B\bar{B}$ MC samples, there is background that peaks in $M_{\rm bc}$ and ΔE (but not $M(D_s^+\pi^0)$) mostly coming from three-body $B \to \bar{D}\pi^0 D_s^+$ decays. This background is modeled in the fits by $M_{\rm bc}$ and ΔE signal functions and a linear function for $M(D_s^+\pi^0)$.

As an example, we show fit results for the $B^0 \to D^- D_{s0}^{*+}$ signal MC sample in the upper part of Fig. 3. The lower part of Fig. 3 shows the results from fits to the generic MC sample. In these figures and subsequent plots in this report, the red short-dashed curve is the fitted background; the green long-dashed curve has the peaking background added and the solid blue curve includes the signal.

The detection efficiencies determined from the signal MC events that survive the application of the multiple event selection requirements are listed in Table II.

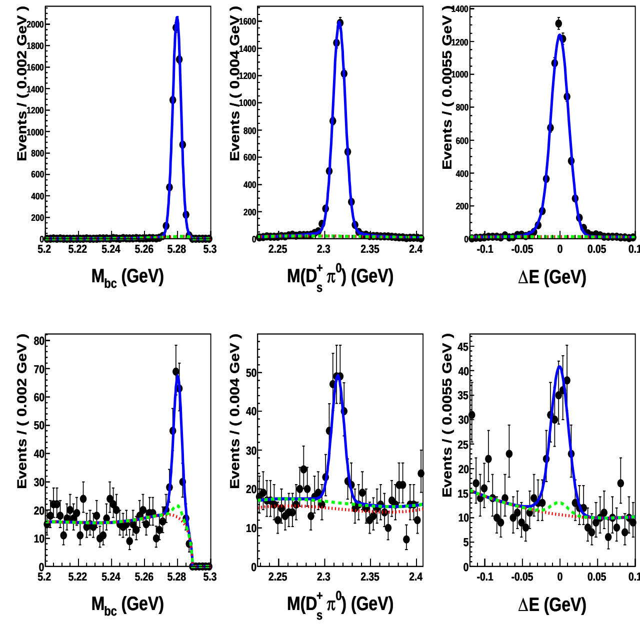

FIG. 3: **Top:** The $M_{\rm bc}$ (left), $M(D_s^+\pi^0)$ (center) and ΔE (right) distributions for the $B^0 \to D^- D_{s0}^{*+}$ signal MC events with the results of the fit superimposed. The events in each distribution are in the signal regions of the two quantities not being plotted. **Bottom:** The corresponding distributions for the generic MC event sample (~ 3 times the data). (See text for curves.)

TABLE II: The MC-determined $B \to \bar{D}D_{s0}^{*+}$ efficiencies.

	$B^0 \to D^- D_{s0}^{*+}$ $D^- \to K^+\pi^-\pi^-$	$B^+ \to \bar{D}^0 D_{s0}^{*+}$ $\bar{D}^0 \to K^+\pi^-$	$B^+ \to \bar{D}^0 D_{s0}^{*+}$ $\bar{D}^0 \to K^+\pi^+\pi^-\pi^-$
$N_{\rm gen}$	266230	266230	266230
$N_{\rm fit}$	7022 ± 90	8575 ± 97	4839 ± 72
effic.	$(2.64 \pm 0.03)\%$	$(3.22 \pm 0.04)\%$	$(1.82 \pm 0.03)\%$

VII. $B \to \bar{D}D_{S0}^{*+}$; $D_{S0}^{*+} \to D_S^+\pi^0$ RESULTS

A. 1) $B^0 \to D^- D_{s0}^{*+}$, $D_{s0}^{*+} \to D_s^+\pi^0$

We determine the number of $B^0 \to D^- D_{s0}^{*+}$; $D_{s0}^{*+} \to D_s^+\pi^0$ signal events in the data by applying the three-dimensional fit described above to the selected $\bar{D} = D^-$ candidates. In this fit, the rms widths of the $M_{\rm bc}$, $M(D_s^+\pi^0)$ and ΔE signal functions are kept fixed at their MC-determined values. Figure 4 shows the results of the fit, which returns a signal yield of $N_{\rm evt} = 102.6^{+12.7}_{-12.0}$ events. The fitted peaking background yield is consistent with zero: 7.7 ± 13.6 events. The signal significance, determined as the square root of twice the difference of log-likelihood values from fits with and without a signal term, is 9.9σ.

We determine the product branching fraction from the

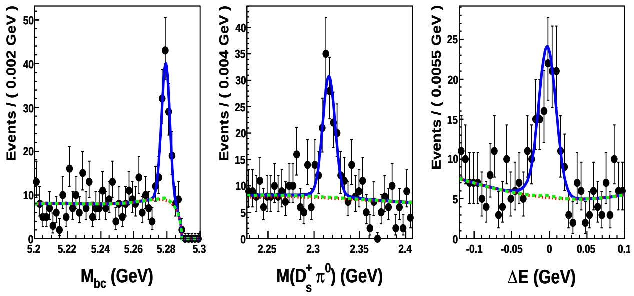

FIG. 4: The $M_{\rm bc}$ (left), $M(D_s^+\pi^0)$ (center) and ΔE (right) distributions for projections of the $B^0 \to D^- D_{s0}^{*+}$ candidate events that are in the signal regions of the two quantities not being plotted. The results of the fit described in the text are superimposed. (See text for curves.)

relation

$$\mathcal{B}(B^0 \to D^- D_{s0}^{*+}) \times \mathcal{B}(D_{s0}^{*+} \to D_s^+\pi^0) = \frac{N_{\rm evt}}{N_{B\bar{B}}\eta_{D^- D_s^+}\mathcal{B}_{D^-}\mathcal{B}_{D_s^+}}, \quad (2)$$

where $N_{B\bar{B}} = (772{\pm}11){\times}10^6$ is the number of $B\bar{B}$ events in the data sample and $\eta_{D^- D_s^+}$ is the MC-determined detection efficiency for this channel (see Table II). The result is

$$\mathcal{B}(B^0 \to D^- D_{s0}^{*+}) \times \mathcal{B}(D_{s0}^{*+} \to D_s^+\pi^0) = (10.2^{+1.3}_{-1.2} \pm 1.0 \pm 0.4) \times 10^{-4}, \quad (3)$$

where (and elsewhere in this report) the first error is statistical, the second is the systematic error (discussed below), and the third reflects the errors on the PDG branching fractions of the D^- and D_s^+ mesons [6]. This result agrees well with the average of the BaBar and previous Belle measurements mentioned above with a substantial improvement in precision.

B. 2) $B^+ \to \bar{D}^0 D_{s0}^{*+}$, $D_{s0}^{*+} \to D_s^+\pi^0$

The top plots of Fig. 5 show the $M_{\rm bc}$, $M(D_s^+\pi^0)$ and ΔE distributions of the $B^+ \to \bar{D}^0 D_{s0}^{*+}$, $D_{s0}^{*+} \to D_s^+\pi^0$, $\bar{D}^0 \to K^+\pi^-$ candidates. Here, in addition to the rms widths, we fix the $M_{\rm bc}$ and ΔE peak positions. The fit results are $38.9^{+9.0}_{-8.2}$ signal events and $12.6^{+22.6}_{-7.7}$ peaking background events. An application of the equivalent of Eq. (2) to this mode results in the product branching fraction

$$\mathcal{B}(B^+ \to \bar{D}^0 D_{s0}^{*+}) \times \mathcal{B}(D_{s0}^{*+} \to D_s^+\pi^0) = (7.5^{+1.7}_{-1.6} \pm 0.7 \pm 0.3) \times 10^{-4}, \quad (4)$$

which is in good agreement with the PDG average of previous measurements but with a smaller error.

The bottom plots of Fig. 5 show the $M_{\rm bc}$, $M(D_s^+\pi^0)$ and ΔE distributions of the $B^+ \to \bar{D}^0 D_{s0}^{*+}$, $D_{s0}^{*+} \to D_s^+\pi^0$, $\bar{D}^0 \to K^+\pi^+\pi^-\pi^-$ candidates. Here again, in addition to the rms widths, we fix the $M_{\rm bc}$ and ΔE peak positions. The fit results are $52.4^{+12.5}_{-11.6}$ signal events and $99.0^{+12.5}_{-19.9}$ peaking background events. An application of the equivalent of Eq. (2) to this mode results in the product branching fraction

$$\mathcal{B}(B^+ \to \bar{D}^0 D_{s0}^{*+}) \times \mathcal{B}(D_{s0}^{*+} \to D_s^+\pi^0) = (8.6^{+2.1}_{-1.9} \pm 1.1 \pm 0.4) \times 10^{-4}, \quad (5)$$

which is in good agreement with the result for the $\bar{D}^0 \to K^+\pi^-$ mode and the PDG average of previous measurements and with a comparable error.

The weighted average of the two measurements is

$$\mathcal{B}(B^+ \to \bar{D}^0 D_{s0}^{*+}) \times \mathcal{B}(D_{s0}^{*+} \to D_s^+\pi^0) = (8.0^{+1.3}_{-1.2} \pm 1.1 \pm 0.4) \times 10^{-4}, \quad (6)$$

where near-complete correlation of the systematic errors for the two measurements is taken into account.

As a consistency check, we apply a simultaneous fit to the two modes, where we find a total signal yield of $91.9^{+15.3}_{-14.6}$ with a statistical significance of 5.9σ. The peaking background yield is $148.5^{+25.7}_{-24.5}$ events. The signal yield from the simultaneous fit is consistent with the sum of individual fits, while the number of peaking background events is marginally higher. The product branching fraction obtained using the simultaneous fit is

$$\mathcal{B}(B^+ \to \bar{D}^0 D_{s0}^{*+}) \times \mathcal{B}(D_{s0}^{*+} \to D_s^+\pi^0) = (8.1^{+1.4}_{-1.3} \pm 1.1 \pm 0.3) \times 10^{-4}, \quad (7)$$

in good agreement with the result from the weighted average of results for each mode.

C. 3) Systematic errors

Systematic errors include the errors on $N_{B\bar{B}}$ and the D and D_s^+ secondary branching fractions, MC statistics and model dependence, MC-data differences in particle identification, charged-particle tracking, π^0 identification, and the choice of the fitting model. The error on $N_{B\bar{B}}$ is 1.4% and the secondary branching fraction relative errors are the PDG values: $D^+ \to K^-\pi^+\pi^+$ (2.0%); $D^0 \to K^-\pi^+$ (1.3%); $D^0 \to K^-\pi^+\pi^+\pi^-$ (2.6%); $D_s^+ \to K^+K^-\pi^+$ (3.9%). The MC model dependence is evaluated by varying the $D_s^+ \to \phi\pi^+$ component of $D_s^+ \to K^+K^-\pi^+$ decays between extreme limits and changing the phase space distributions for the multibody D-meson decay modes. We use various control samples to determine MC-data efficiency differences that are common to many Belle analyses to evaluate systematic errors associated with: kaon (pion) identification of 1.1% per track (1.2% per track); charged particle tracking of 0.35% per track; and π^0 detection of 4.0%.

The dependence on the fitting model is estimated from changes observed by redoing the fits with each parameter fixed at $\pm 1\sigma$ from its best-fit value. The systematic

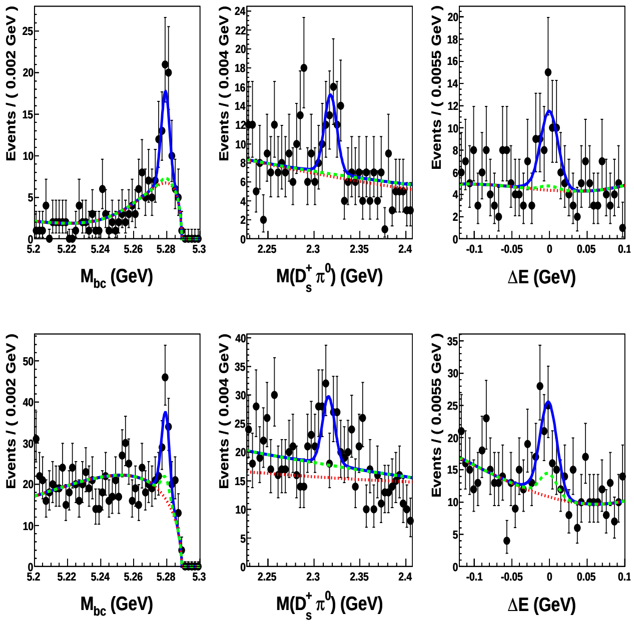

FIG. 5: **Top:** The $M_{\rm bc}$ (left), $M(D_s^+\pi^0)$ (center) and ΔE (right) distributions for the $B^+ \to \bar{D}^0 D_{s0}^{*+}$ candidate events for the $\bar{D}^0 \to K^+\pi^-$ sub-decay mode, with the results of the fit superimposed. The events in each distribution are in the signal regions of the two quantities not being plotted. **Bottom:** The corresponding distributions for $\bar{D}^0 \to K^+\pi^+\pi^-\pi^-$ decays. (See text for curves.)

errors from each source, listed in Table III, are summed in quadrature to get the final value.

TABLE III: Summary of relative systematic error sources (in percent).

	$B^0 \to D^- D_{s0}^{*+}$ $D^- \to K\pi\pi$	$B^+ \to \bar{D}^0 D_{s0}^{*+}$ $\bar{D}^0 \to K\pi$	$B^+ \to \bar{D}^0 D_{s0}^{*+}$ $\bar{D}^0 \to K3\pi$
D&D_s^+ BFs	4.4	4.1	4.7
$N_{B\bar{B}}$	1.4	1.4	1.4
MC model dep.	3.6	2.3	5.9
MC stat.	1.2	1.0	1.4
Particle ID	6.9	5.2	8.4
Tracking	2.1	1.8	2.5
Fit params.	4.4	5.8	4.7
π^0	4.0	4.0	4.0
Quad. sum	10.2	9.4	12.4

VIII. SEARCH FOR $\mathbf{z}^{++} \to D_S^+\pi^+$ AND $\mathbf{z}^0 \to D_S^+\pi^-$

We look for $\mathbf{z}^{++} \to D_s^+\pi^+$ and $\mathbf{z^0} \to D_s^+\pi^-$ signals in the $B^+ \to D^- D_s^+\pi^+$ and $B^0 \to \bar{D}^0 D_s^+\pi^-$ decay channels by applying the selection criteria discussed above with the replacement of the selected π^0 with a π^+ (for $\mathbf{z}^{++}$) or π^- (for $\mathbf{z^0}$). Here, for events with multiple $\bar{D}$ and/or D_s^+ track combinations, we select those with a measured invariant mass closest to the corresponding PDG values. For $\mathbf{z}^{++}$ signal MC, the number of remaining events with multiple candidates is 11.2% over the full three-dimensional range of the likelihood fit; for $\mathbf{z^0}$, fewer than 0.1% of the remaining events have multiple candidates.

A. 1) Peaking backgrounds from generic MC samples

We check for possible peaking backgrounds leaking into the signal using a sample of simulated generic B-meson decay events (with no $\mathbf{z}^{++}$ nor $\mathbf{z^0}$ signals) with a luminosity that corresponds to three times the number of B decays in the data. The top plots of Fig. 6 show the results of applying the three-dimensional fit to selected $D^- D_s^+\pi^+$ MC events. Here, the signal yield is zero with a positive error of 7.1 events. The peaking background yield is 544 ± 41 events. The middle (bottom) plots of Fig. 6 show the results of the three-dimensional fits to the generic MC for the $\bar{D}^0 \to K^+\pi^-$ ($\bar{D}^0 \to K^+\pi^+\pi^-\pi^-$) channel in the selected $B \to \mathbf{z^0}\bar{D}^0$ samples. No background processes are found that produce a spurious signal; the signal yields are also zero for both $\bar{D}^0$ modes with positive errors of 2.1 and 9.9 events for the $K^+\pi^-$ and $K^+\pi^+\pi^-\pi^-$ modes, respectively. The $M_{\rm bc}$-ΔE peaking background yields for these modes are 169 ± 22 and 229^{+32}_{-31} events, respectively.

B. 2) Mass-dependent efficiency

Since the $\mathbf{z}^{++}$ and $\mathbf{z^0}$ are hypothesized to be isospin partners of the D_{s0}^{*+}, their masses are expected to lie somewhere within a ± 10 MeV mass region of $m_{D_{s0}^{*+}} = 2317.8 \pm 0.6$ MeV. In order to be certain that we cover all reasonably plausible mass values, we scan for $\mathbf{z}^{++}$ and $\mathbf{z^0}$ signals in 13 adjacent mass bins, each 5 MeV wide, covering a ± 32.5 MeV interval centered on 2317.8 MeV.

To account for possible mass dependence of the detection efficiency, we generate $\mathbf{z}^{++}$ and $\mathbf{z^0}$ signal MC events with $\mathbf{z}$ masses in the full range of the scan. The efficiencies, determined from fits to the selected events from each MC sample, are independent of mass to within the $\sim$2.5% MC statistical errors. For the $\mathbf{z}^{++}$ search, the average efficiency is (8.3 ± 0.1)%. For the $\mathbf{z^0}$ search, the average efficiency is (9.2 ± 0.1)% for the $\bar{D}^0 \to K^+\pi^-$ mode and (4.1 ± 0.1)% for $\bar{D}^0 \to K^+\pi^+\pi^-\pi^-$.

C. 3) Fits to the $M(D_s^+\pi^{+,-})$ spectra

We apply a sequence of 13 three-dimensional fits to the data using a Gaussian signal function with width fixed at

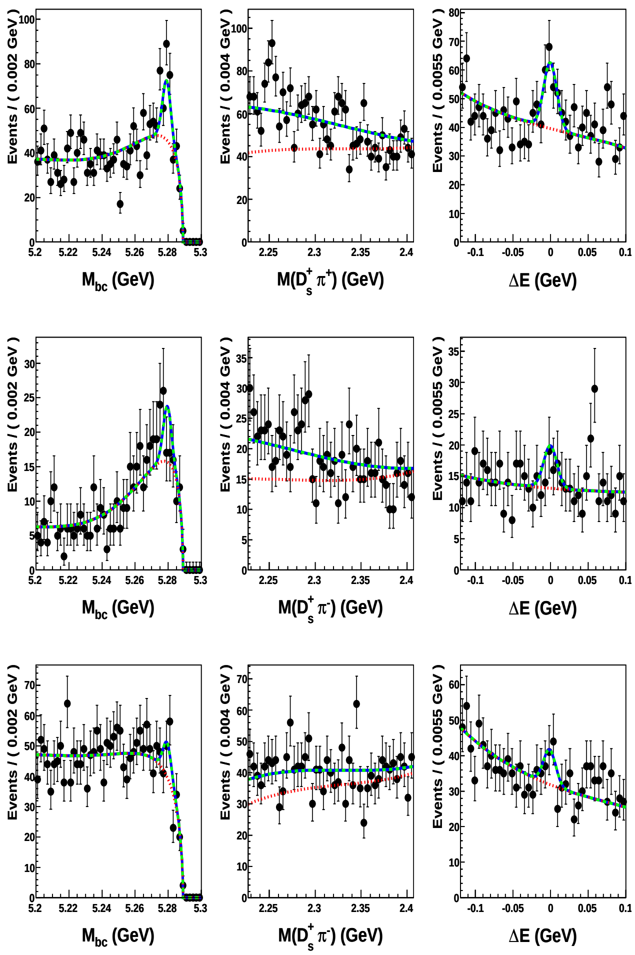

FIG. 6: The $M_{\rm bc}$ (left), $M(D_s^+\pi)$ (center) and ΔE (right) distributions for generic-MC events that pass the $D^- D_s^+\pi^+$ (top), $\bar{D}^0 D_s^+\pi^-$, $\bar{D}^0 \to K^+\pi^-$ (middle) and $\bar{D}^0 D_s^+\pi^-$, $\bar{D}^0 \to K^+\pi^+\pi^-\pi^-$ (bottom) channels. The curves are the results of fits described in the text.

the MC-determined $D_s^+\pi^\pm$ mass resolution (σ=4.6 MeV) to represent the $\mathbf{z}^{++}$ ($\mathbf{z^0}$) with a peak mass restricted to 5 MeV-wide windows covering a total mass range of $\pm$32.5 MeV about $m_{D_{s0}^{*+}}$ = 2317.8 MeV. The results of these fits for the $\mathbf{z}^{++} \to D_s^+\pi^+$ and $\mathbf{z^0} \to D_s^+\pi^-$ searches are summarized in Table IV. As examples, we show the fit results for the mass bin centered at $M(D_s^+\pi)$ = 2317.8 MeV for the $\mathbf{z}^{++}$ ($\mathbf{z^0}$) search in the top (bottom) plots of Fig. 7. None of the fits returns a positive $\mathbf{z}^{++}$ or $\mathbf{z^0}$ signal with a statistical significance of more than 1.3σ. The determination of the Bayesian 90% credibility level upper limits [26] on the event yields and product branching fractions is described below.

TABLE IV: Product branching fraction upper limits $\mathcal{B}_i^{\rm UL}$ for $\mathcal{B}(B^+\ (B^0)\ \to D^-\ (\bar{D}^0)\ z_i) \times \mathcal{B}(z_i\ \to D_s^+\pi\ )$ ($z_1 = \mathbf{z}^{++}$ and $z_2 = \mathbf{z^0}$), for z_i masses between 2285.3 MeV and 2350.3 MeV. Here $\Delta M = M_{\rm ctr} - m_{D_{s0}^{*+}}$, where $M_{\rm ctr}$ is the center of the 5 MeV mass window allowed for the fit, and $N_i^{\rm UL}$ is the upper limit including systematic errors.

ΔM MeV	$N_{++}^{\rm fit}$	$N_{++}^{\rm UL}$	$\mathcal{B}_{++}^{\rm UL}$ (10^{-4})	$N_0^{\rm fit}$	$N_0^{\rm UL}$	$\mathcal{B}_0^{\rm UL}$ (10^{-4})
-30	$4.0^{+5.9}_{-9.0}$	16.3	0.52	-13.7 ± 6.2	10.5	0.34
-25	$4.1^{+5.9}_{-5.9}$	16.3	0.52	$5.5^{+7.9}_{-15.6}$	21.2	0.69
-20	$-8.3^{+5.3}_{-4.2}$	9.8	0.32	$5.8^{+8.0}_{-8.2}$	21.5	0.69
-15	$-10.3^{+4.0}_{-3.1}$	8.0	0.25	2.7 ± 8.3	20.1	0.65
-10	-10.2 ± 3.5	7.9	0.25	$4.0^{+7.9}_{-8.4}$	20.4	0.66
-5	-8.8 ± 3.2	8.1	0.25	4.1 ± 7.4	20.4	0.66
0	-9.3 ± 3.0	8.4	0.27	$3.1^{+7.8}_{-7.9}$	19.8	0.64
5	$-9.3^{+4.5}_{-3.0}$	8.5	0.28	$-1.7^{+10.3}_{-6.1}$	16.0	0.52
10	$4.6^{+5.6}_{-10.8}$	16.2	0.51	$-5.4^{+7.6}_{-5.3}$	13.4	0.44
15	6.4 ± 5.0	17.8	0.57	$-5.4^{+6.7}_{-5.3}$	13.3	0.43
20	$6.0^{+5.9}_{-5.1}$	17.6	0.56	$-3.3^{+11.5}_{-5.6}$	14.3	0.47
25	$3.0^{+6.9}_{-5.9}$	15.8	0.50	$5.7^{+7.2}_{-6.9}$	20.6	0.67
30	$3.4^{+5.7}_{-5.6}$	15.8	0.50	$5.6^{+7.0}_{-5.1}$	20.0	0.65

D. 4) Systematic errors for $\mathbf{z}^{++}$ and $\mathbf{z^0}$ searches

Systematic errors are evaluated using the same methods that are used for the D_{s0}^{*+} branching fraction measurement described above, with the π^0-associated error replaced by the error on the additional charged pion. For this, the nominal 0.35% tracking error is assigned to $p > 200$ MeV tracks. However, 5% of the relevant pions for the $\mathbf{z^0}$ have $p < 200$ MeV with an associated error of 5%. Here, a weighted average is used and the total tracking uncertainty increases to 3.8%. For the systematic error associated with multiple candidates, we perform a multiple-candidate-free $\mathbf{z}^{++}$ scan where we use the smallest ΔE to select the best candidate and a two-dimensional fit ($M_{\rm bc}$ and $M(D_s^+\pi^+)$) to measure signal yields. From the differences between the results of the two methods, we determine a systematic error from this source of 2.2%. For other sources of error, we use the results listed in Table III. The resulting errors are 11.4% for the $\mathbf{z}^{++}$ search and 16.6% for the $\mathbf{z^0}$ search.

E. 5) Upper limit determination

We use a Bayesian method to convert the fitted results to upper limits on the total number of signal events. To account for the systematic uncertainties, the likelihood distributions from the $\mathbf{z}^{++}$ ($\mathbf{z^0}$), fits are convolved with a Gaussian with $\sigma_{\rm syst} = 0.114\ (0.166) \times N_{\rm stat}^{\rm UL}$, where $N_{\rm stat}^{\rm UL}$ is determined from

$$\frac{\int_0^{N_{\rm stat}^{\rm UL}} \mathcal{L}(n_{\rm sig}) dn_{\rm sig}}{\int_0^{+\infty} \mathcal{L}(n_{\rm sig}) dn_{\rm sig}} = 0.9. \tag{8}$$

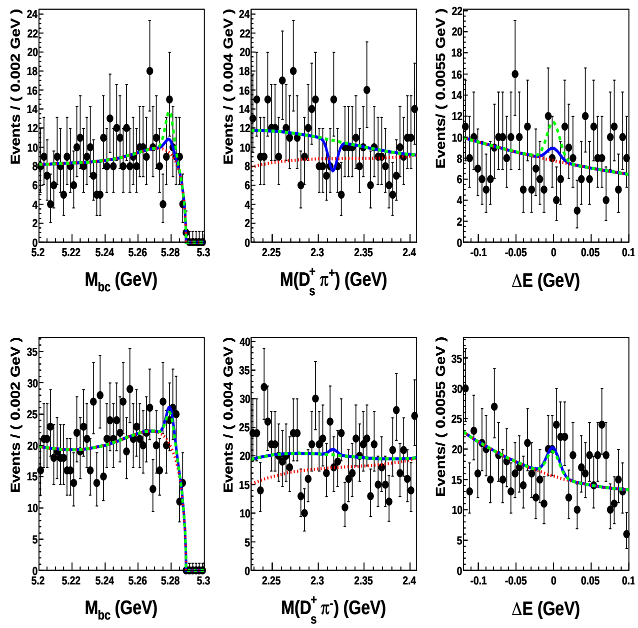

FIG. 7: The $M_{\rm bc}$ (left), $M(D_s^+\pi)$ (center) and ΔE (right) distributions for selected $B^+ \to D^- D_s^+\pi^+$ (top) and $B^0 \to \bar{D}^0 D_s^+\pi^-$ (bottom) event candiates for the fit with the signal peak mass restricted to a 5 MeV region centered at $M(D_s^+\pi) = 2317.8$ MeV. In the lower plots, the $\bar{D}^0 \to K^+\pi^-$ and $K^+\pi^+\pi^-\pi^-$ samples are combined. (See text for curves.)

The Gaussian width is $\sigma_{\rm syst} = 1.1$ (3.1) events for the 2317.8 MeV mass bin of the $\mathbf{z}^{++}$ ($\mathbf{z^0}$) scan; the widths for the other mass bins are similar. The corresponding upper limits, $N^{\rm UL}$, are determined from the relation

$$\frac{\int_0^{N^{\rm UL}} \mathcal{L}(n_{\rm sig}) \bigotimes \mathcal{G}(n_{\rm sig}) dn_{\rm sig}}{\int_0^{+\infty} \mathcal{L}(n_{\rm sig}) \bigotimes \mathcal{G}(n_{\rm sig}) dn_{\rm sig}} = 0.9, \tag{9}$$

and in all cases differ from $N^{\rm UL}_{\rm stat}$ by less than one event. The resulting values of $N^{\rm UL}$ are listed in Table IV.

For the $\mathbf{z}^{++}$ search, we determine upper limits on the product branching fractions $\mathcal{B}^{\rm UL}_{++} \equiv \mathcal{B}(B \to D^- \mathbf{z}^{++}) \times \mathcal{B}(\mathbf{z}^{++} \to D_s^+\pi^+)$ from the relation

$$\mathcal{B}^{\rm UL}_{++} = \frac{N^{\rm UL}_{++}}{N_{B\bar{B}} \mathcal{B}_{D_s^+} \mathcal{B}_{D^-} \eta_{++}}, \tag{10}$$

where the notation follows that of Eq. (2) and η_{++} is the MC-determined efficiency. For the $\mathbf{z^0}$ search, where there is no evidence for the signal either, we use the same relation with $\mathcal{B}_{D^-}\eta_{++}$ replaced by $\mathcal{B}_{K\pi}\eta_{K\pi} + \mathcal{B}_{K3\pi}\eta_{K3\pi}$, where $\eta_{K\pi}$ ($\eta_{K3\pi}$) is the efficiency for the $\bar{D}^0 \to K^+\pi^-$ ($K^+\pi^+\pi^-\pi^-$) mode. The resulting product branching fraction upper limits, listed in Table IV, are all more than an order of magnitude lower than the measured values for the $\bar{D}D_{s0}^{*+}$ final states. This is in strong contradiction to expectations for the hypothesis that the D_{s0}^{*+} is a member of an isospin triplet [16].

IX. SUMMARY

We report measurements of the product branching fractions $\mathcal{B}(B^+ \to \bar{D}^0 D_{s0}^{*+}) \times \mathcal{B}(D_{s0}^{*+} \to D_s^+\pi^0) = (8.0^{+1.3}_{-1.2} \pm 1.1 \pm 0.4) \times 10^{-4}$ and $\mathcal{B}(B^0 \to D^- D_{s0}^{*+}) \times \mathcal{B}(D_{s0}^{*+} \to D_s^+\pi^0) = (10.2^{+1.3}_{-1.2} \pm 1.0 \pm 0.4) \times 10^{-4}$. Here, the first errors are statistical, the second are systematic and the third are from D and D_s^+ branching fractions. These values agree with the existing PDG world average values [6], significantly improve upon their precision, and supersede those of Ref. [4]. In addition, we report negative results on a search for hypothesized doubly charged and neutral isospin partners of the D_{s0}^{*+} and provide upper limits on the product branching fractions that are more than an order of magnitude smaller than the theoretical predictions of Hayashigaki and Terasaki [16].

X. ACKNOWLEDGMENTS

We thank the KEKB group for the excellent operation of the accelerator; the KEK cryogenics group for the efficient operation of the solenoid; and the KEK computer group, the National Institute of Informatics, and the PNNL/EMSL computing group for valuable computing and SINET4 network support. We acknowledge support from the Ministry of Education, Culture, Sports, Science, and Technology (MEXT) of Japan, the Japan Society for the Promotion of Science (JSPS), and the Tau-Lepton Physics Research Center of Nagoya University; the Australian Research Council and the Australian Department of Industry, Innovation, Science and Research; Austrian Science Fund under Grant No. P 22742-N16 and P 26794-N20; the National Natural Science Foundation of China under Contracts No. 10575109, No. 10775142, No. 10875115, No. 11175187, and No. 11475187; the Ministry of Education, Youth and Sports of the Czech Republic under Contract No. LG14034; the Carl Zeiss Foundation, the Deutsche Forschungsgemeinschaft and the VolkswagenStiftung; the Department of Science and Technology of India; the Istituto Nazionale di Fisica Nucleare of Italy; National Research Foundation (NRF) of Korea Grants No. 2011-0029457, No. 2012-0008143, No. 2012R1A1A2008330, No. 2013R1A1A3007772, No. 2014R1A2A2A01005286, No. 2014R1A2A2A01002734, No. 2014R1A1A2006456; the Basic Research Lab program under NRF Grant No. KRF-2011-0020333, No. KRF-2011-0021196, Center for Korean J-PARC Users, No. NRF-2013K1A3A7A06056592; the Brain Korea 21-Plus program and the Global Science Experimental Data Hub Center of the Korea Institute of Science and Technology Information; the Institute of Basic Science (Korea) Project Code IBS-DR016-D1; the Polish Ministry of Science and Higher Education and the National Science Center; the Ministry of Education and Science of the Russian Federation and the Russian Foundation for Basic Research; the Slovenian Research Agency; the

Basque Foundation for Science (IKERBASQUE) and the Euskal Herriko Unibertsitatea (UPV/EHU) under program UFI 11/55 (Spain); the Swiss National Science Foundation; the National Science Council and the Ministry of Education of Taiwan; and the U.S. Department of Energy and the National Science Foundation. This work is supported by a Grant-in-Aid from MEXT for Science Research in a Priority Area ("New Development of Flavor Physics") and from JSPS for Creative Scientific Research ("Evolution of Tau-lepton Physics").

[1] B. Aubert *et al.* (BaBar Collaboration), Phys. Rev. Lett. **90**, 242001 (2003).

[2] In this report the inclusion of charge-conjugate states is always implied.

[3] D. Besson *et al.* (CLEO Collaboration), Phys. Rev. D **68**, 032002 (2003).

[4] P. Krokovny *et al.* (Belle Collaboration), Phys. Rev. Lett. **91**, 262002 (2003).

[5] B. Aubert *et al.* (BaBar Collaboration), Phys. Rev. Lett. **93**, 181801 (2004).

[6] K.A. Olive *et al.* (Particle Data Group), Chin. Phys. C **38**. 090001 (2014). The signal MC data to get efficiencies was generated using particle branching fractions taken from the PDG2012 tables: J. Beringer *et al.* (Particle Data Group), Phys. Rev. D **86**, 010001 (2012).

[7] We use the convention that $c = 1$.

[8] S. Godfrey and N. Isgur, Phys. Rev. D **32**, 189 (1985); S. Godfrey and R. Kokoski, Phys. Rev. D **43**, 1679 (1991); S.N. Gupta and J.M. Johnson, Phys. Rev. D **51**, 168 (1995); J. Zeng, J.W. Van Orden and W. Roberts, Phys. Rev. D **52**, 5229 (1995); D. Ebert, V.O. Galkin and R.N. Faustov, Phys. Rev. D **57**, 5663 (1998); M. Di Pierro and E. Eichten, Phys. Rev. D **64**, 114004 (2001); Y.S. Kalishnikova, A.V. Nefediev and A. Simonov, Phys. Rev. D **64**, 014037 (2001); D. Merten, R. Ricken, M. Koll, B. Metsch and H. Petry, Eur. Phys. J. A **13**, 477 (2002); and W. Lucha and F.F. Schröberl, Mod. Phys. Lett. A **13**, 2837 (2003).

[9] S. Boyle *et al.* (UKQCD Collaboration), Nucl. Phys. Proc. Suppl. **63**, 314 (1998); G.S. Bali, Phys. Rev. D **68**, 071501(R) (2003); and A. Dougall *et al.* (UKQCD Collaboration), Phys. Lett. B **569**, 41 (2003).

[10] T. Barnes, F.E. Close and H.J. Lipkin, Phys. Rev. D **68**, 054006 (2003); and A.P. Szczepaniak, Phys. Lett. B **567**, 23 (2003).

[11] V. Dmitrasinovic, Phys. Rev. Lett. **94**, 162002 (2003); and H.-Y. Cheng and W.-S. Hu, Phys. Lett. B **566**, 193 (2003).

[12] E. van Beveran and G. Rupp, Phys. Rev. Lett. **91**, 012003 (2003); T.E. Browder, S. Pakvasa and A.A. Petrov, Phys. Lett. B **578**, 365 (2004); and D. Mohler, C.B. Lang, L. Leskovec, S. Prelovsek and R.M. Woloshyn, Phys. Rev. Lett. **111**, 222001 (2013).

[13] T. Mehen and R.P. Springer, Phys. Rev. D **70**, 074014 (2004); P. Colangelo and F. De Fazio, Phys. Lett B **570**, 180 (2003) and W.A. Bardeen, E.J. Eichten and C.T. Hill, Phys. Rev. D **68**, 054024 (2003).

[14] A. Datta and P.J. O'Donnell, Phys. Lett. B **572**, 164 (2003).

[15] B.-H. Chen and H.-n. Li, Phys. Rev. D **69**, 054002 (2004).

[16] A. Hayashigaki and K. Terasaki, Prog. Theor. Phys. **14**, 1191 (2005).

[17] B. Aubert *et al.* (BaBar Collaboration), Phys. Rev. D **74**, 032007 (2006).

[18] K. Terasaki, Prog. Theor. Phys. **14**, 1191 (2005).

[19] S. Kurokawa and E. Kikutani, Nucl. Instr. and Meth. A **499**, 1 (2003), and other papers included in this volume; T. Abe *et al.*, Prog. Theor. Exp. Phys. **2013**, 03A001 (2013) and references therein.

[20] A. Abashian *et al.* (Belle Collaboration), Nucl. Instr. and Meth. A **479**, 117 (2002), Y. Ushiroda (Belle SVD2 Group), Nucl. Instr. and Meth. A **511**, 6 (2003), and J. Brodzicka *et al.*, Prog. Theor. Exp. Phys. **2012**, 04D001 (2012) and references therein.

[21] E. Nakano *et al.* (Belle Collaboration), Nucl. Instr. and Meth. A **494**, 402 (2002).

[22] G.C. Fox and S. Wolfram, Phys. Rev. Lett. **41**, 1581 (1978).

[23] Events are generated with the EvtGen generator, D.J. Lange, Nucl. Instr. and Meth. A **462**, 152 (2001) and the detector response is simulated with GEANT, R. Brun *et al.*, GEANT 3.21, CERN Report DD/EE/84-1, 1984.

[24] H. Albrecht *et al.* (ARGUS Collaboration), Phys. Lett. B **229**, 304 (1989).

[25] T. Skwarnicki, Ph.D. Thesis, Institute for Nuclear Physics, Krakow 1986; DESY Internal Report, DESY F31-86-02 (1986).

[26] Common convention has used the frequentist label "confidence level" for this criterion.